Version of Record: https://www.sciencedirect.com/science/article/pii/S0378779622006411
Manuscript_76cc04d733642e5c89986a775ad528c7

Stochastic Model Predictive Controller for Wind Farm Frequency Regulation in Waked Conditions

Sunny Chen, Johanna L. Mathieu, Peter Seiler
Department of Electrical Engineering and Computer Science
University of Michigan, Ann Arbor, MI, USA
{chensunn, jlmath, pseiler}@umich.edu

***Abstract*—As renewable energy penetrations increase, wind farms may be required to provide ancillary services such as frequency regulation. For wind farms, two issues complicate frequency regulation: turbine-wake interactions alter the available wind power, and the future power reference signal is uncertain. This paper presents a stochastic model predictive controller (MPC) for wind farms to track an uncertain frequency regulation signal while accounting for wakes. The controller uses a simplified Park model with wake propagation delay to predict turbine-wake interactions. The controller operates without any knowledge of the future power regulation signal or wind speed. The controller solves a nonconvex stochastic optimization program using scenario optimization. Our stochastic MPC tracks with 7-10% less error than our deterministic MPC controllers.**

***Index Terms*—frequency regulation, stochastic model predictive control, wind farm control**

I. Introduction

Currently, wind farms are operated to maximize their energy production. However, as wind energy replaces traditional power generating resources, wind farms may be called on to provide ancillary services such as frequency regulation, in which a power plant tracks a power reference command that varies on the timescale of seconds. When providing frequency regulation, wind farms are usually forced to curtail their average power production in order to increase power when requested. Curtailment results in lost revenue and reduces the economic viability of the farm [1]. However, derating a turbine also increases the energy content in its wake. The extra energy in the flow field allows the wind farm to temporarily extract more power downstream if necessary. Hence, by carefully allocating turbine power generation when frequency regulation calls for a reduction in power production, it is possible to reduce the amount of curtailment required for reference tracking. In fact, it is possible to use knowledge of the future frequency regulation signal to transiently track signals that exceed the maximum steady-state power obtainable from the wind by reducing power in anticipation of a frequency regulation signal increase. However, in practice, the future frequency regulation signal is not known. This is the issue we aim to address.

This paper develops model predictive controllers for wind farms to track a frequency regulation signal without knowledge of the future reference signal. The controller uses a Park model with wake propagation delay to predict wake interactions between turbines. To deal with uncertainty in the power reference signal, we employ forecasts of the power reference, an objective function that maximizes the total available power at each time step, and stochastic optimization using an asymmetric objective function.

Prior work in wind farm control for frequency regulation has focused on developing control-oriented wake models and actuation schemes that use axial induction and wake steering. One approach for wind farm power reference tracking is to dispatch each turbine to produce power proportional to the turbine's available power, as shown in [2]. Ref. [3] also uses this approach in an MPC controller that uses both axial induction and wake steering but does not account for wake dynamics. Ref. [4] expands on [3] by introducing a stochastic MPC controller that accounts for uncertain wind through scenario-based optimization. Ref. [5] describes a distributed MPC approach to follow a power reference through adjusting axial induction and wake steering. The proportional allocation approach does not account for turbine wakes and allocates turbine power suboptimally. Another approach is to employ MPC with a wind farm wake model to issue optimized commands. Ref. [6] develops a control-oriented wake model for use in a model predictive controller that tracks better and requires less derate than controllers without a wake model. Ref. [7] presents a controller that dispatches turbines to track a reference while heuristically minimizing the power deficits from wakes. These approaches can allocate wind power while minimizing turbine wakes, but they do not account for an unknown future power reference. Finally, [8] employs an ARMA model to forecast a regulation signal as part of an MPC reference tracking controller for distributed energy resources. We follow a similar approach for our forecast. From this literature review, we conclude that no work in wind farm frequency regulation explicitly treats the future power reference as unknown.

The contributions of this paper are: 1) the development of deterministic MPC controllers that leverage wake models and forecasts of the power reference signal; 2) the development of a stochastic MPC controller which uses an objective that asymmetrically penalizes underproduction of power in future timesteps; and 3) case studies on a wind farm with significant waking and unknown future power reference. The case studies compare the performance of the deterministic and stochastic

This work was supported by NSF Grant 1845093, NYSERDA Project 147503, and a Rackham Merit Fellowship.

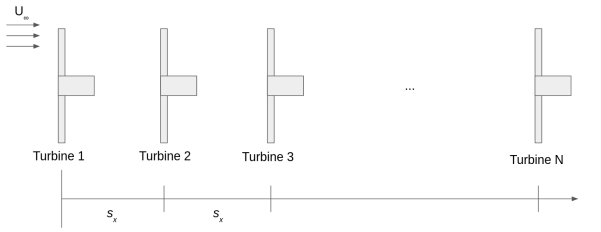

Fig. 1. Diagram of the wind farm considered in this paper.

formulations; in particular, we analyze tracking performance and how the controllers allocate turbine power production.

The remainder of this paper is organized as follows. Section II introduces and motivates the problem. Section III describes the wake model used in our controller. Section IV outlines our MPC power tracking framework. Section V contains results from case studies in which we simulate our controller on both a derated and non-derated farm. Section VI gives our conclusion and remarks on future work.

II. Problem Description

In this paper, we consider the problem of minimizing the error between a wind farm's total power generation and a power reference generated from a system operator's frequency regulation signal (e.g., PJM's RegD signal). The farm we consider consists of a string of N identical turbines aligned with the wind direction, as shown in Fig. 1; $\mathcal{N} = \{1, \ldots, N\}$ is the set of turbine indices. We assume that adjacent turbines are equally spaced by distance s_x. Let $P_{\text{dem}}(k)$ be the wind farm power output demanded by frequency regulation signal $r(k) \in [-1, 1] \ \forall k$, and let $P_{\text{gen}}(k)$ be the total power generation of the wind farm, all at timestep k. The wind farm calculates $P_{\text{dem}}(k)$ as a shift and scaling of $r(k)$ using $P_{\text{dem}}(k) = P_{\text{MPP}}[1 - \Delta P + M \cdot r(k)]$, where P_{MPP} is the maximum power point of the farm (i.e., the maximum power that can be generated by the farm in steady-state), ΔP is the level of farm derate, and M is the magnitude of the frequency regulation power. Then, we aim to minimize

$$\sum_{k=1}^{T_{\text{horz}}} (P_{\text{gen}}(k) - P_{\text{dem}}(k))^2 \tag{1}$$

where $\mathcal{K} = \{1, 2, \ldots, T_{\text{horz}}\}$ is the time horizon. The problem is formulated in discrete-time with sample time Δt set to 2 seconds, consistent with the timestep of PJM's RegD signal.

It is difficult for a wind farm to track a power reference because: 1) turbine wakes dynamically alter the available power; 2) the frequency regulation signal (which captures both the frequency deviation from the nominal frequency due to supply-demand mismatch and unscheduled tieline flows between separately managed portions of the grid) is unknown for future timesteps, and; 3) the wind speed changes over time and is uncertain. In this paper, we design our controller to handle 1) and 2), but not 3). Although our work could conceivably be extended to handle uncertainty in wind speed, we neglect 3) in order to focus on managing the uncertainty in the frequency regulation signal. We also assume that the wind speed does not affect the frequency regulation signal, although in reality the frequency regulation signal may change due to supply-demand mismatch resulting from wind forecast error. Other works, e.g., [6], also assume constant freestream wind speed.

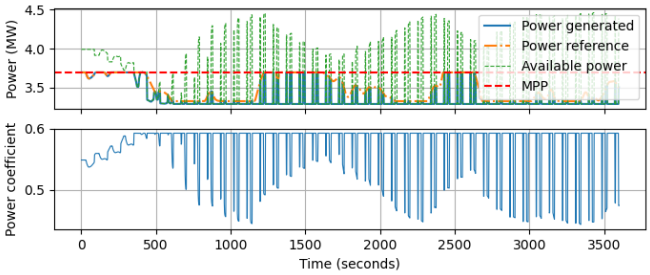

Fig. 2. Reference tracking without a wake model or reference forecast.

We next provide motivating examples that justify the need for our approach. Then we analyze frequency regulation signals and their forecastability.

A. Motivating Examples

In this section, we present examples to show why we model the wake and forecast the power reference signal. First, we consider a naive power reference tracking controller that does not use a wake model or forecast. It commands each turbine to capture the same proportion of its available local wind power. We assume that the controller knows the local wind speed and wind power at each turbine, and that the controller minimizes the squared-error between power generation and the reference power at the current timestep.

Fig. 2 shows results from running the naive controller on an hour-long power reference. The top plot displays the power generated, power reference, available power, and maximum power point (MPP) of the wind farm, while the bottom plot displays the power coefficient of each turbine. The available power is the maximum instantaneous power that the farm can produce at a given time, while the MPP is the maximum steady-state power. Note that the power reference never surpasses the MPP. At the beginning of the simulation, the controller increases the farm's power output. The turbines experience lower local wind speeds due to upstream wakes, causing the available power to drop. In response, the controller maximizes the power generation, but it generally cannot track the signal due to turbine wakes. The available power oscillates due to wake coupling introduced by dips in the power reference. The turbines can derate to meet the power need occasionally, but the controller still fails to track due to its greedy behavior.

Fig. 3 shows the results from reference tracking leveraging a wake model and with full knowledge of the reference signal over the entire horizon. We select control commands that minimize the tracking error over the constraints imposed by the wake model; the full details of this approach are given in Section IV. The controller uses foreknowledge of the power reference to preemptively "store" power by slightly derating

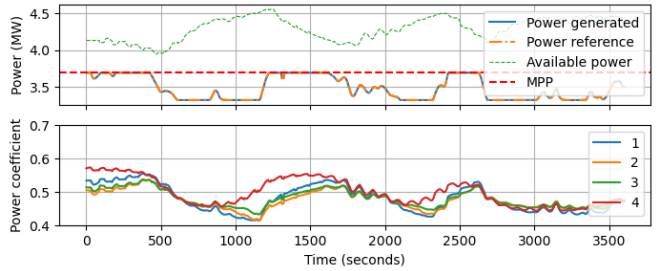

Fig. 3. Reference tracking with a wake model and a perfect reference forecast.

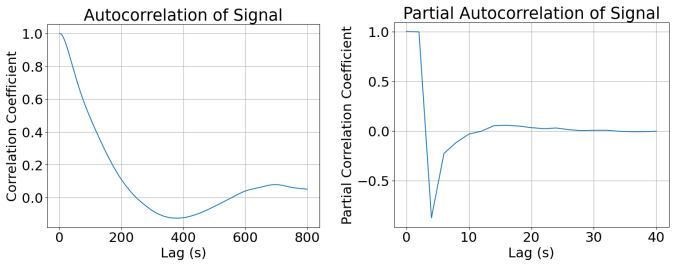

Fig. 4. Autocorrelation and partial autocorrelation of PJM's RegD signal.

turbines, for example at $t = 1000$ seconds. The controller is able to track the power reference without error.

These examples underscore the importance of considering the effects of wakes and also managing power reference uncertainty. Our goal is to design a controller that properly harnesses wake interactions to achieve performance as close as possible to that in Fig. 3, but without full knowledge of the reference signal. We do this by employing an MPC approach that optimizes the turbine power outputs using a wake model and forecasts of the power reference signal.

B. Regulation Signal Analysis

Since in practice we do not know the future power reference signal, we must create a forecast to use a predictive control approach. Here, we highlight statistical features of the regulation signal $r(k)$ that enable us to forecast. We use PJM Regulation Signal Data from PJM [9]. To create the RegD signal, PJM high-pass filters the area control error (ACE) which captures frequency deviations (resulting from supply-demand mismatch), unscheduled tieline flows, and time error [10]. Essentially, frequency regulation corrects the mismatch between supply and demand resulting from forecast error, which makes the frequency regulation signal itself inherently difficult to forecast. However, we observe that there is still some autocorrelation within the signal over short timespans. Fig. 4 contains plots of the autocorrelation and partial autocorrelation functions of the sample signal. The signal exhibits significant correlation for lags up to about 200 seconds, after which the correlation goes approximately to 0. Additionally, the partial autocorrelation of the signal cuts off at about 3 lags. This justifies the use of an autoregressive (AR) model, i.e., an AR(3) model, to forecast the signal.

III. Wake Model

We next describe the wake model we use in our controller formulation. The axial induction factors for each turbine serve as our control inputs. The axial induction factor measures the velocity deficit induced by the turbine in the wind. Although the axial induction is not directly a turbine control input, a turbine can be made to track a given axial induction through manipulation of its blade pitch and generator torque. Let $a_i(k)$ denote the axial induction factor for turbine i at timestep k. The corresponding power coefficient (by Betz theory [11]) is

$$C_P(a_i(k)) = 4a_i(k) \cdot (1 - a_i(k))^2. \tag{2}$$

The power coefficient is the proportion of power captured by the turbine from the available energy within the wind. From Betz theory, $a_i(k) \in [0, 1/3]$ and $C_P(a_i(k)) \in [0, 0.593]$. The power captured by turbine i at timestep k is

$$P_{\text{turb},i}(k) = \min\left(P_{\text{rated}},\ \frac{1}{2}\left(\frac{\pi D^2}{4}\right)\rho\, C_P(a_i(k))\ (u_i(k))^3\right), \tag{3}$$

where D is the turbine rotor diameter, ρ is the air density, $u_i(k)$ is the local wind speed for turbine i at timestep k, and P_{rated} is the maximum (rated) power of each turbine.

We model the wind speed within the farm using a Park model with wake propagation times [12] [13]. The local wind speed at turbine 1 is the freestream velocity $u_1(k) = U_\infty$. In this paper, we assume U_∞ is constant over time. The local wind speed at downstream turbines ($i = 2, \ldots, N$) is reduced by wake effects, i.e.,

$$u_i(k) = U_\infty\ [1 - \delta V_i(k)\ ], \tag{4}$$

where $\delta V_i(k)$ is the velocity deficit of turbine i at timestep k. The deficit is defined using a square-superposition of the past control actions of upstream turbines [13]

$$\delta V_i(k) = 2\sqrt{\sum_{j=1}^{i-1}[c_{i,j}a_j(k - d_{i,j}))]^2}, \tag{5}$$

where $c_{i,j}$ is a constant describing the coupling between turbines i and j, and $d_{i,j}$ is the wake propagation delay time between turbines i and j. The constant $c_{i,j}$ is $\left(\frac{D}{D+2\kappa_e s_{i,j}}\right)^2$, where κ_e is the wake expansion constant and $s_{i,j}$ is the turbine separation distance between turbines i and j. The turbine spacing is a constant s_x and hence $s_{i,j} = |j - i|s_x$. Moreover, the delay in units of sample times is $d_{i,j} = |j - i|d$ where d is the delay between adjacent turbines, i.e., $\lceil \frac{s_x}{U_\infty \Delta t} \rceil$. These equations give the physical connection between the actions (axial induction) of an upstream turbine on the delayed downstream wind speed.

IV. Controller Design

In this section, we describe our MPC approach. An MPC controller employs a predictive model of the plant over a horizon with an objective function corresponding to the goal of the control. At each timestep, the controller solves an optimization problem with the plant model and the objective, then implements the control actions from the current timestep only; this procedure is repeated at every timestep with updated

state and forecast information. We use MPC because it allows us to directly optimize control actions over a wake model.

Each MPC iteration optimizes over a T-length horizon $\{k_0, k_0+1, \ldots, k_0+T-1\}$, where k_0 denotes the initial timestep of the horizon within $\mathcal{K}$. However, within each horizon, the MPC optimization objective is only run on the timesteps $k_0, k_0+d, \ldots, k_0+N_{\text{wakes}}d$, where N_{wakes} is the number of wake propagations within the horizon. We can discard variables outside of these timesteps because we only implement only the control command at k_0, and k_0's wake only affects timesteps k_0+d, k_0+2d, etc. Thus, we restrict each iteration to the timesteps $\mathcal{K}_{k_0} = \{k_0, \ldots, k_0+N_{\text{wakes}}d\}$.

Different power system operators use different metrics to evaluate the performance of resources providing frequency regulation. Here, we simply quantify performance using (1), i.e., the squared error between $P_{\text{dem}}(k)$ and $P_{\text{gen}}(k)$. Since $P_{\text{dem}}(k)$ is unknown for future timesteps, we instead construct alternative references $P_{\text{ref}}(k)$ and $\widetilde{P}_{\text{ref}}(k)$. Deterministic reference signal $P_{\text{ref}}(k)$ equals $P_{\text{dem}}(k)$ at the current timestep $k=k_0$, but is a forecast $P_{\text{forecast}}(k)$ for $k>k_0$. Stochastic reference signal $\widetilde{P}_{\text{ref}}(k)$ is defined at timesteps $k>k_0$ and treats future timesteps as random variables.

Vectors $\mathbf{a}$ and $\mathbf{x}$ contain the axial induction and state variables of each turbine at each timestep, respectively, i.e.,

$$\mathbf{a} = \begin{bmatrix} a(k_0)^\top & \ldots & a(k_0+N_{\text{wakes}}d)^\top \end{bmatrix}, \tag{6}$$

$$\mathbf{x} = \begin{bmatrix} \delta V(k_0)^\top & \ldots & \delta V(k_0+N_{\text{wakes}}d)^\top \end{bmatrix}, \tag{7}$$

where $a(k)$ and $\delta V(k)$ contain the N axial inductions and wake velocity deficits at timestep k. The state variables give the wind velocity deficits at each turbine. Finally, the vector $\mathbf{r}$ consists of previous values of $P_{\text{dem}}(k)$, i.e.,

$$\mathbf{r} = \begin{bmatrix} P_{\text{dem}}(1) & P_{\text{dem}}(2) & \ldots & P_{\text{dem}}(k_0) \end{bmatrix}^\top. \tag{8}$$

Our MPC controller uses $\mathbf{r}$ to form power reference forecasts.

A. Objective Functions

We compare the performance of several different objective functions in our MPC formulation. Although we are trying to minimize (1), we use different objectives that accommodate uncertain power references. The first objective function we use is the mean-squared error (MSE)

$$J_1(\mathbf{a},\mathbf{x},\mathbf{r}) = \frac{1}{|\mathcal{K}_{k_0}|}\sum_{k\in\mathcal{K}_{k_0}} \left(P_{\text{ref}}(k) - P_{\text{gen}}(k)\right)^2. \tag{9}$$

We can augment J_1 with a second term, referred to as a "power maximization" term, following the approach in [7]

$$J_2(\mathbf{a},\mathbf{x},\mathbf{r}) = -\sum_{k\in\mathcal{K}_{k_0}}\sum_{i=1}^{N}(u_i(k))^3. \tag{10}$$

Since $(u_i(k))^3$ is proportional to the available power, minimizing (10) incentivizes forward turbines to lower their power production to minimize the wake effect on back turbines. This allows the farm to track higher power reference commands at future timesteps.

Our third objective function is used in the stochastic MPC. First, consider the following asymmetric MSE loss function

$$f_{\text{asym}}(x_1,x_2) = \begin{cases} (x_1-x_2)^2, & \text{for } x_1 > x_2, \\ 0, & \text{for } x_1 \le x_2. \end{cases} \tag{11}$$

This loss function is positive only when x_1 is greater than x_2. We employ this asymmetric loss function in our full objective function as follows:

$$J_3(\mathbf{a},\mathbf{x},\mathbf{r}) = \left(P_{\text{dem}}(k_0) - P_{\text{gen}}(k_0)\right)^2 + \mathbb{E}\left[\sum_{k\in\mathcal{K}_{k_0}} f_{\text{asym}}(\widetilde{P}_{\text{ref}}(k), P_{\text{gen}}(k))\right]. \tag{12}$$

This objective only imposes a penalty on underproducing, not overproducing, power during future timesteps. We use this asymmetric loss function for two reasons. First, preparing to overproduce power in the future is not problematic. If the farm prepares to overproduce but the power is lower than forecasted, then the farm can derate to meet the reference. If the farm does not prepare to overproduce, then the future available power may be insufficient to track. Second, using a symmetric MSE loss in stochastic MPC does not improve on deterministic MPC with a point forecast. It is equivalent to minimize the expected MSE loss with a random signal and the MSE loss using a point forecast. On the other hand, the expected value of the asymmetric objective varies with the uncertainty of the stochastic signal. When solving, we approximate the objective function using an approach that considers a finite number of scenarios for the reference signal

$$\widetilde{J}_3(\mathbf{a},\mathbf{x},\mathbf{r}) = \left(\widetilde{P}_{\text{ref}}(k_0) - P_{\text{gen}}(k_0)\right)^2 + \frac{1}{N_s}\sum_{s=1}^{N_s}\left[\sum_{k\in\mathcal{K}_{k_0}} f_{\text{asym}}(P_{\text{scen},s}(k), P_{\text{gen}}(k))\right], \tag{13}$$

where N_s is the number of scenarios and $P_{\text{scen},s}(k)$ is a realization of $\widetilde{P}_{\text{ref}}(k)$, i.e., a scenario.

B. Deterministic MPC

The optimization problem run at each iteration is

$$\min_{\mathbf{a}} \ \gamma\, J_1(\mathbf{a},\mathbf{x},\mathbf{r}) + (1-\gamma)\, J_2(\mathbf{a},\mathbf{x}) \tag{14}$$

$$\text{s.t. } 0.05 \le a_i(k) \le 1/3,\ \forall i \in \mathcal{N}\setminus N, \forall k \in \mathcal{K}_{k_0} \tag{15}$$

$$a_N(k) = 1/3,\ \forall k \in \mathcal{K}_{k_0} \tag{16}$$

$$|a_i(k_0) - a_i(k_0-1)| \le \delta a \tag{17}$$

$$P_{\text{gen}}(k) = \sum_{i=1}^{N} P_{\text{turb},i}(k),\ \forall k \in \mathcal{K}_{k_0} \tag{18}$$

$$\text{(2)-(5)},\ \forall i \in \mathcal{N}, \forall k \in \mathcal{K}_{k_0},$$

where (14) minimizes the squared tracking error in J_1 and maximizes the available power in J_2; the weighting between these two objectives is specified by γ. Eq. (15) constrains $\mathbf{a}$ and (16) constrains the rearmost turbine to maximize its power production. The rearmost turbine's uncaptured wind

power does not travel to another turbine and cannot be recovered. So, the back turbine should maximize its power. This restriction also reduces the number of decision variables in the optimization problem, making it easier to solve. Eq. (17) constrains the ramp rate of $\mathbf{a}$ to be less than a constant δa. Eq. (18) defines the generated power at any timestep to be the sum of the power capture of each turbine. Eqs. (2)-(5) encode the wake behavior and turbine power capture characteristics.

As previously described, $P_{\text{ref}}(k)$ contains a forecast of the signal for timesteps $k \geq k_0$. We employ four different forecasts throughout this paper: 1) persistence forecast, 2) worst-case forecast, 3) autoregressive forecast, and 4) perfect forecast. The persistence forecast $P_{\text{forecast}}(k)$ equals $P_{\text{dem}}(k_0),\ \forall k \in \mathcal{K}_{k_0}$. The worst-case forecast $P_{\text{forecast}}(k)$ equals $P_{\text{high}},\ \forall k \in \mathcal{K}_{k_0}$, where P_{high} is $P_{\text{MPP}}[1-\Delta P+M]$, i.e. the highest power demand possible. The controller with worst-case forecast plans for high future power demand because the controller can derate if the power is less than forecasted. In the autoregressive forecast, $P_{\text{dem}}(k)$ is forecasted with an AR(3) model with parameters ϕ_m, for $m = 1, 2, 3$. To forecast $k = k_0 + 1$,

$$P_{\text{forecast}}(k) = \sum_{m=1}^{3} \phi_m P_{\text{dem}}(k-m). \tag{19}$$

Successive timesteps are forecasted using $P_{\text{forecast}}(k)$ instead of $P_{\text{dem}}(k)$ when $P_{\text{dem}}(k)$ is unknown. Finally, the perfect forecast $P_{\text{forecast}}(k)$ corresponds to $P_{\text{forecast}}(k) = P_{\text{dem}}(k),\ \forall k \in \mathcal{K}_{k_0}$. The perfect forecast is used as a benchmark for other forecasts. The second motivational example in Section II was generated by solving a single iteration of the deterministic MPC using a perfect forecast and an MPC horizon equal to the problem time horizon T_{horz}.

C. Stochastic MPC

The stochastic MPC uses the same constraints as the deterministic MPC but uses the stochastic objective in (12). The optimization problem run at each iteration is

$$\begin{aligned} \min_{\mathbf{a}}\ & \widetilde{J}_3(\mathbf{a}, \mathbf{x}, \mathbf{r}) \\ \text{s.t. } & (15)\text{-}(18), \\ & (2)\text{-}(5),\ \forall i \in \mathcal{N}, \forall k \in \mathcal{K}_{k_0}, \end{aligned} \tag{20}$$

where (20) is the approximate asymmetric loss function (13).

In the stochastic MPC, the power reference scenarios are drawn from the AR(3) model used in the autoregressive forecast. To generate the scenarios, we simulate the model with white noise innovations $\epsilon_k \sim \mathcal{N}(0, \sigma^2)$ such that

$$\widetilde{P}_{\text{ref}}(k) = \sum_{m=1}^{3} \phi_m P_{\text{dem}}(k-m) + \epsilon_k, \tag{21}$$

where σ^2, the white noise variance, is found by fitting data.

TABLE I
SIMULATION PARAMETERS

Parameter	Value
ρ, Air density	1.223 kg/m^3
D, Rotor diameter	100 m
U_∞, Freestream wind velocity	8 m/s
P_{rated}, Rated power	3 MW
κ_e, Wake expansion coefficient	0.05
s_x, Turbine spacing	700 m
N_s, Number of stochastic scenarios	50 samples
δa, Ramp rate constrant	0.02

V. RESULTS AND DISCUSSION

We test the controller's performance for a variety of prediction horizon lengths, farm configurations, and reference signals. Our simulation parameters are listed in Table I. We use half of the PJM power reference data [9] to fit the autoregressive model and the other half to run simulations. For a given controller configuration, we calculate the controller's root mean squared error (RMSE) and normalized root mean squared error (NRMSE) by conducting 8 trials on different hour-long reference signals. The same reference signals are used among each controller configuration. The RMSE is defined as $(\sum_{k=1}^{T_{\text{horz}}}(P_{\text{gen}}(k)-P_{\text{dem}}(k))^2/T_{\text{horz}})^{\frac{1}{2}}$ and the NRMSE is defined as $\text{RMSE}/(P_{\text{MPP}}[1-\Delta P]) \cdot 100\%$.

In each MPC iteration, we solve a nonlinear and nonconvex optimization problem. We modeled the problem using Julia JuMP, then solved it using IPOPT with the HSL MA97 linear solver [14] [15] [16]. The solver is not guaranteed to converge to the global minimum.

A. Forecast Error

We begin by quantifying the forecast accuracy to better compare the different MPC options. We calculate the RMSE of each forecast on 50 regulation signal samples of varying lengths and compare the mean and standard deviations of the RMSEs. The regulation signal is normalized between -1 and $+1$ and is thus unitless. Table IV contains our results, which show that the worst-case forecast has considerably more error than the persistence or autoregressive forecasts. The autoregressive and persistence forecasts have similar mean RMSEs, but the autoregressive forecast has less variance in the RMSE, especially as the horizon length increases. Based on these results, we expect that controllers using the autoregressive forecast will have the least tracking error, controllers using the worst-case forecast will have the most tracking error, and controllers using the persistence forecast will have tracking error in between the errors of the other two forecasts.

B. Control of a Derated Farm

We first present a set of trials on a 4-turbine farm with $\Delta P = 0.04$ (4% derate) and $M = 0.08$ (8% signal magnitude). Since the derate is less than the signal magnitude, the controller must take advantage of aerodynamic effects to track the reference signal well. Table II contains error results for all combinations of objective functions and forecasts, as well as the optimal prediction length (OPL) for the given objective

TABLE II
RMSE AND NRMSE FROM DERATED FARM

Objective	Forecast	RMSE (kW)	NRMSE (%)	OPL (wakes)
MSE	Persistence	8.31	0.234	1
	Worst-case	8.52	0.240	1
	Autoregressive	8.09	0.228	2
	Perfect	6.40	0.180	6
MSE + Power max.	Persistence	8.42	0.237	1
	Worst-case	8.65	0.244	1
	Autoregressive	8.28	0.234	2
	Perfect	5.31	0.150	2
Asymmetric	Stochastic	7.52	0.212	2

TABLE III
RMSE AND NRMSE FROM NON-DERATED FARM

Objective	Forecast	RMSE (kW)	NRMSE (%)	OPL (wakes)
MSE	Persistence	40.90	1.107	4
	Worst-case	36.56	0.989	3
	Autoregressive	44.09	1.193	6
	Perfect	33.70	0.912	6
MSE + Power max.	Persistence	36.89	0.998	3
	Worst-case	35.56	0.962	2
	Autoregressive	35.04	0.948	6
	Perfect	24.93	0.675	6
Asymmetric	Stochastic	32.5	0.880	6

TABLE IV
FORECAST RMSE MEAN AND STANDARD DEVIATION

Forecast	RMSE Statistic	Horizon length (timesteps) 46	91	136	181	226	271
Persistence	Mean	0.32	0.48	0.56	0.61	0.64	0.68
	STD	0.25	0.29	0.32	0.31	0.30	0.28
Worst-case	Mean	1.08	1.09	1.13	1.15	1.16	1.15
	STD	0.51	0.46	0.43	0.42	0.39	0.36
Autoregressive	Mean	0.30	0.42	0.50	0.52	0.54	0.56
	STD	0.19	0.20	0.17	0.18	0.16	0.14

function and forecast. Fig. 5 compares three controllers with different objective functions run on the same reference: 1) MSE objective (9) with autoregressive forecast; 2) MSE + Power maximization term (10) with autoregressive forecast; 3) asymmetric objective (12) with stochastic MPC. The prediction lengths for each controller are set to their optimal values in Table II. Fig. 5a displays the power generated, power reference, available power, and MPP for each of these controllers, while the bottom plot displays the axial induction commanded to each turbine for each controller. We do not display the axial induction of the fourth turbine because it is constant and equal to $1/3$ for all controllers.

The results in Table II show that the deterministic MPC with autoregressive forecast outperforms both the persistence and worst-case forecasts. We note the tracking error decreases as the forecast mean and standard deviation (displayed in Table IV) decrease. In turn, the stochastic MPC with asymmetric objective function outperforms the autoregressive forecast, but performs worse than the perfect forecast. Table II also shows that including the power maximization term generally worsens the tracking performance when the farm is derated. When the farm is derated, the controller naturally experiences higher wind speeds due to decreased waking, so the power maximization term does not improve tracking.

The controllers in Fig. 5a cannot track the signal well in the first 10 minutes because there is not enough available power in the flow field. The axial inductions in Fig. 5b show that the stochastic controller harvests less power initially so that it can track better around minutes 7 and 8. Fig. 5b also shows that the power maximization controller allocates more power to the front turbine and less to the back turbines, while the MSE and asymmetric controllers command similar axial inductions to the front turbine. However, the asymmetric controller is less aggressive in the back turbines.

C. Control of a Non-Derated farm

We now present trials where the farm is not derated and the signal magnitude is 4%. Since the farm is not derated, the controller must carefully account for wake coupling effects so that the farm can overproduce power. Table III contains error results across all combinations of forecasts and controllers. All controllers perform worse on the non-derated farm compared to the derated farm because the average power demanded is higher in the non-derated case. When considering the controllers that use the MSE objective, we see that the controller with the worst-case forecast outperforms both the persistence and autoregressive forecast. This is likely because the worst-case forecast incentivizes the controller to reduce wake coupling effects, which allows it to surpass the MPP more often. We note that, across all forecast methods, using the power maximization term lowers tracking error compared to the MSE objective. This is likely because maintaining higher available power is more difficult when the farm is not derated. Additionally, for the power tracking objective, improving the forecast (as shown in Table IV) also reduces the tracking error. Finally, the stochastic controller outperforms the persistence, worst-case, and autoregressive forecast, but does worse than the perfect forecast with power maximization term.

Fig. 6 again compares the controllers used in Fig. 5. We change the prediction lengths to match those in Table III. When comparing Fig. 6a to Fig. 5a, we see that in both farms, controllers struggle to track when the power reference exceeds P_{MPP}. However, the non-derated farm can overproduce power for less time compared to the derated farm, leading to its worse tracking performance. Fig. 6b indicates that on the non-derated farm, the stochastic and power maximization controllers allocate more power to the front turbines, while the MSE controller allocates power more evenly among the turbines. Since the power maximization term reduces error for this signal, it makes sense for the asymmetric controller to mimic the power maximization controller.

Our results show that the stochastic controller performs better than our other controllers on both the derated and non-derated farm configurations. The stochastic MPC can explicitly account for the level of uncertainty in the forecasts, whereas

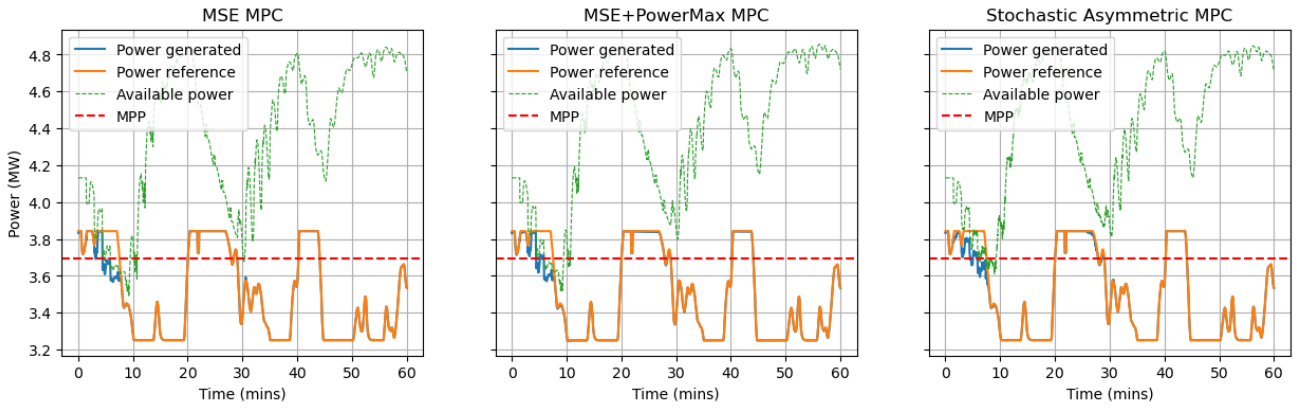

(a) Comparison of power generated from derated farm using different objective functions.

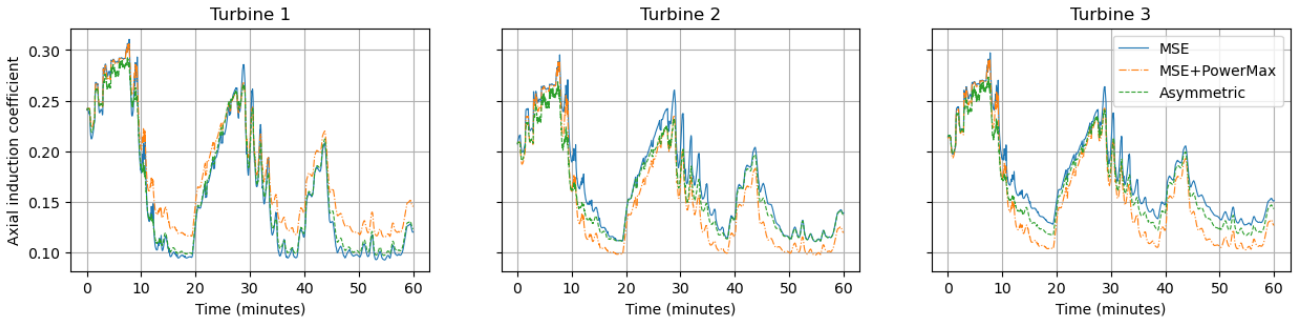

(b) Axial induction commands from controller using different objective functions on derated farm.

Fig. 5. Calculated axial induction for derated 4-turbine farm using different objective functions.

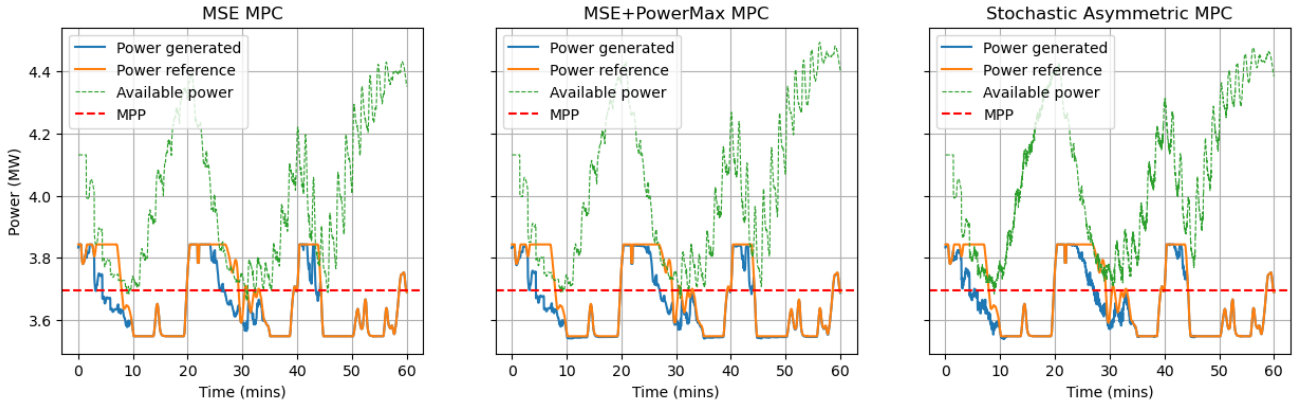

(a) Comparison of power generated from non-derated farm using different objective functions.

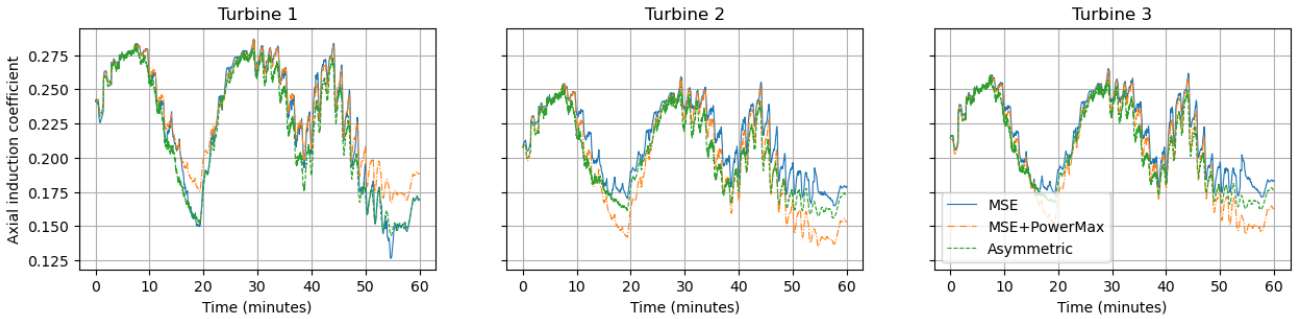

(b) Axial induction commands from controller using different objective functions on non-derated farm.

Fig. 6. Calculated axial induction for non-derated 4-turbine farm using different objective functions.

the deterministic MPC has only a point forecast and thus cannot adjust its actions based on uncertainty.

D. Controller Runtime

In this section, we present representative runtime results for the controller. Fig. 7 contains a log-log plot of the runtime per iteration of the deterministic and stochastic MPC controllers for a 4 and 10 turbine farm with varying prediction horizon length. These results show that although the stochastic controller is slower than the deterministic controller, the time per iteration for both is considerably less than the sample time of 2 seconds. This holds even as the farm size increases to 10 turbines.

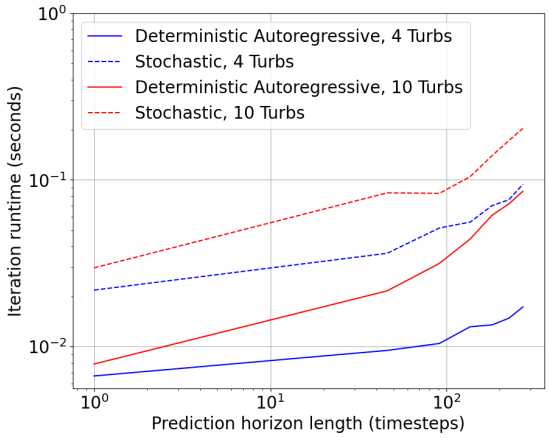

Fig. 7. Log-log plot of runtime per iteration for 4 and 10 turbine farm.

VI. Conclusion and Future Work

We have developed an MPC framework to efficiently allocate turbines for power reference tracking under power reference uncertainty. First, we use forecasts to predict future periods of high power production. Second, we employ alternative objective functions to find solutions that both minimize the tracking error and maximize the future power flexibility of the wind farm. These predictions allow the controller to preemptively "store" more energy in the flow field to meet higher demands in the future. Although the frequency regulation signal is hard to forecast, we found that controllers using an AR model of the power reference signal outperformed controllers using a persistence or worst-case forecast.

Our future work will include improvements in model fidelity and controller evaluation. Here, we only simulate the controller on farm layouts where the turbines are aligned with the wind direction and the wake effect is maximized. We need to extend and verify our work for realistic farm layouts with partial waking. Additionally, in this work, our controller's wake model is the same model used for simulation. To better verify the efficacy of our controller, we need to test the controller in more realistic simulations, e.g., SimWindFarm. We could also extend our controller with more realism, such as using a Gaussian wake model, modeling deep array effects, including turbine dynamics, and incorporating wind uncertainty. These are areas that would add more fidelity to our controller models and simulations. We also wish to consider turbine mechanical loading in our model. Mechanical loads contribute to farm operations and maintenance costs, so including loading would provide us with a better sense of the economic consequences of our control strategy. Finally, we hope to provide theoretical grounding for using the asymmetric objective function in the stochastic MPC.

References

[1] S. Rose and J. Apt, "The cost of curtailing wind turbines for secondary frequency regulation capacity," *Energy Systems*, vol. 5, no. 3, pp. 407–422, Sep. 2014.

[2] A. D. Hansen, P. Sørensen, F. Iov, and F. Blaabjerg, "Centralised power control of wind farm with doubly fed induction generators," *Renewable Energy*, vol. 31, no. 7, pp. 935–951, Jun. 2006.

[3] S. Boersma, V. Rostampour, B. Doekemeijer, W. van Geest, and J.-W. van Wingerden, "A constrained model predictive wind farm controller providing active power control: an LES study," *Journal of Physics: Conference Series*, vol. 1037, p. 032023, 2018.

[4] S. Boersma, B. M. Doekemeijer, T. Keviczky, and J. W. v. Wingerdenl, "Stochastic model predictive control: uncertainty impact on wind farm power tracking," in *American Control Conference*, 2019, pp. 4167–4172.

[5] C. J. Bay, J. Annoni, T. Taylor, L. Pao, and K. Johnson, "Active power control for wind farms using distributed model predictive control and nearest neighbor communication," in *2018 Annual American Control Conference (ACC)*, 2018, pp. 682–687, ISSN: 2378-5861.

[6] C. R. Shapiro, P. Bauweraerts, J. Meyers, C. Meneveau, and D. F. Gayme, "Model-based receding horizon control of wind farms for secondary frequency regulation: Model-based receding horizon control for frequency regulation," *Wind Energy*, vol. 20, no. 7, pp. 1261–1275, Jul. 2017.

[7] S. Siniscalchi-Minna, M. De-Prada-Gil, F. D. Bianchi, C. Ocampo-Martinez, and B. D. Schutter, "A multi-objective predictive control strategy for enhancing primary frequency support with wind farms," *Journal of Physics: Conference Series*, vol. 1037, p. 032034, Jun. 2018.

[8] S. Brahma, A. Khurram, H. Ossareh, and M. Almassalkhi, "Optimal Frequency Regulation using Packetized Energy Management," Jul. 2021, arXiv: 2107.12939.

[9] "PJM - Ancillary Services." [Online]. Available: https://www.pjm.com/markets-and-operations/ancillary-services.aspx

[10] C. Pilong, "PJM Manual 12: Balancing Operations," Aug. 2014. [Online]. Available: https://www.pjm.com/-/media/training/nerc-certifications/gen-exam-materials/manuals/m12v31-balancing-operations.ashx?la=en

[11] T. Burton, Ed., *Wind energy handbook*, 2nd ed. Chichester, West Sussex: Wiley, 2011.

[12] N. Jensen, "A note on wind generator interaction," Risø National Laboratory, Roskilde, Report 87-550-0971-9, 1983.

[13] I. Katic, J. Højstrup, and N. O. Jensen, "A simple model for cluster Efficiency," in *European Wind Energy Association Conference and Exhibition*, 1986, pp. 407–410.

[14] I. Dunning, J. Huchette, and M. Lubin, "Jump: A modeling language for mathematical optimization," *SIAM Review*, vol. 59, no. 2, pp. 295–320, 2017.

[15] A. Wächter and L. T. Biegler, "On the implementation of an interior-point filter line-search algorithm for large-scale nonlinear programming," *Mathematical Programming*, vol. 106, no. 1, pp. 25–57, Mar. 2006.

[16] "HSL. A collection of Fortran codes for large scale scientific computation." [Online]. Available: http://www.hsl.rl.ac.uk/